NANOSYSTEMS:
PHYSICS, CHEMISTRY, MATHEMATICS

Original article

Lebedev V.T., et al. *Nanosystems: Phys. Chem. Math.*, 2024, **15** (5), 716–725.
http://nanojournal.ifmo.ru
DOI 10.17586/2220-8054-2024-15-5-716-725

Ionic channel structure in perfluorinated membranes studied by small angle X-ray scattering, optical and Mössbauer spectroscopy

Vasily T. Lebedev[1,a], Valery S. Kozlov[1,b], Mikhail V. Remizov[1,c], Yury V. Kulvelis[1,d], Oleg N. Primachenko[2,e], Elena A. Marinenko[2,f], Georgy S. Peters[3,g]

[1]Petersburg Nuclear Physics Institute named by B. P. Konstantinov of National Research Center "Kurchatov Institute", Gatchina, Russia

[2]Institute of Macromolecular Compounds, Russian Academy of Sciences, St. Petersburg, Russia

[3]National Research Center "Kurchatov Institute", Moscow, Russia

[a]lebedev_vt@pnpi.nrcki.ru, [b]kozlov_vs1@pnpi.nrcki.ru, [c]m.remizov97@gmail.com, [d]kulvelis_yv@pnpi.nrcki.ru, [e]alex-prima@mail.ru, [f]emarinenkospb@gmail.com, [g]georgspeters@gmail.com

Corresponding author: Vasily T. Lebedev, lebedev_vt@pnpi.nrcki.ru

PACS 81.07.Nb, 82.35.Rs

ABSTRACT Small angle X-ray scattering optical and Mössbauer spectroscopy has been used to study ionic channels in perfluorinated Nafion®-type membranes. X-ray scattering data have revealed the ordering of ionic groups of polymer chains at nanoscales into extended fine channels for proton conductivity. Then the membranes were saturated with Fe^{3+} ions to probe their interaction with sulfonic groups. This remarkably changed electron properties of copolymer in which the energy of optical gap has decreased. The Mössbauer spectra have confirmed that even at ambient temperature in membrane, Fe^{3+} ions are assembled into antiferromagnetic dimers with water shells and associated with sulfonic groups at the channel surfaces. The applied complementary methods allowed us to examine a short-range order of ionic groups forming a network of channels in membranes that provide their functional properties in hydrogen fuel cells.

KEYWORDS ion, channel, membrane, structure, gamma-spectroscopy

ACKNOWLEDGEMENTS The work was supported by the Russian Science Foundation under Grant No. 23-23-00129. The authors thank Professor V. G. Semenov for methodological help, Engineers I. N. Ivanova, L. I. Lisovskaya for technical assistance.

FOR CITATION Lebedev V.T., Kozlov V.S., Remizov M.V., Kulvelis Yu.V., Primachenko O.N., Marinenko E.A., Peters G.S. Ionic channel structure in perfluorinated membranes studied by small angle X-ray scattering, optical and Mössbauer spectroscopy. *Nanosystems: Phys. Chem. Math.*, 2024, **15** (5), 716–725.

1. Introduction

The crucial problem of hydrogen power industry is related to the creation of solid polyelectrolytes serving as ion-exchange membranes for proton transport in fuel cells [1–3]. Presently these key materials are mainly based on Nafion® and Aquvion® perfluorinated copolymers which provide necessary functional characteristics of membranes (proton conductivity, strength, mechanical and thermal stability, low fuel crossover) [4–7]. The ways of the following improvement of these materials cannot be found without a detail analysis of their complicated nanostructure [8–11] which is formed as a result of the segregation of nonpolar chain fragments (partially crystallized) from ionic groups forming narrow pores and channels for water and proton transport [12–18].

Despite of various studies [8–18] of membranes based of perfluorinated copolymers, the present knowledge of self-assembly regularities of ionic groups still remains not satisfactory and various models of their package into channel networks are discussed [11]. Mostly these models propose a formation of nano-sized pores (few nanometers) covered with ionic groups and connected via fine channels ($\sim$ 1 nm in diameter) occluded by nonpolar chain fragments and partially ordered in polymer matrices [8–11].

To understand the subtle features of molecular ordering in membranes, the X-ray and neutron small angle scattering methods (SAXS, SANS) [9–11] along with electron and atomic force microscopy (TEM, SEM, AFM) are used [19–23]. In addition, the Mössbauer (gamma-resonance) spectroscopy (MS) has been applied [24–26] to examine ion-exchange membranes and search for their channel structure, charge states of ions, local symmetry and nearest environment of ions, their magnetic interactions with neighboring atoms, local mobility when ions are bound to hydrophilic polymer fragments. The MS data makes it possible to judge the local heterogeneity of functional groups distribution, in particular, sulfonic

acid groups, which ensure ion exchange in membrane channels. MS in combination with electron microscopy and X-ray diffraction are indispensable methods for studying the relationship between the structure and functional properties of ionomers as the main materials of proton-conducting membranes – key elements of hydrogen fuel cells. [27–29].

The authors [30] analyzed the chemical state and microstructure of Nafion® membranes using EXAFS and MS methods when replacing protons in ionic groups with iron ions by saturating the membranes with iron salts and further drying the samples. The introduction of iron ions ($\sim$ 1 wt.%) into membrane films made it possible to perform the MS experiments at low temperatures (80 and 4.2 K) for measuring isomeric shifts and quadrupole splitting of absorption lines showed the oxidation degree of iron cations in membrane channels. The analysis of the spectral profile for the X-ray absorption near edge spectroscopy (XANES) confirmed a local ordering of iron ions surrounded by oxygen shells at the distance of 0.2 nm due to the formation of $Fe(H_2O)_6^{2+}$ and $Fe(H_2O)_6^{3+}$ complexes when the membranes were saturated with $FeSO_4$ or $FeCl_3$ salts. In perfluorinated ionomers with iron additive the MS has revealed the specificity of aggregation of ionogenic groups that led to the formation of conducting channels in membranes and determined their functional properties.

The ionomers in perfluorinated membranes [31] have a complex morphology, since their sulfonic acid groups, together with counterions, form nanoscale aggregates that ensure physical cross-linking of polymer chains [32,33]. For this reason, a cation exchange may significantly modulate chemical, physical and functional properties of ionomers, change their glass transition temperature, Young's modulus, chain mobility [32–38], permeability, transport and gas separation efficiency [39] due to the influence of cations on pristine material [40].

A modification of Nafion® membranes by exchanging H^+ ions for Fe^{3+} cations was undertaken [40] to limit the mobility of chain segments with cationic crosslinks, increase its resistance to unwanted plasticization by gas mixtures, and increase the rigidity of chains through ionic interactions between Fe^{3+} cations and sulfonate anions, and ultimately, to improve a diffusion selectivity of material. The MS experiments are able to give a detail information on the structure of channels when introduced ions with Mössbauer [41] serve as tiny local probes to study membranes. Except of fundamental interests, there are some technical reasons to analyze the interactions of polyvalent iron with ion exchange membranes, e.g. to predict their fouling and find strategies to combat it. This motivated authors [42] to study the sorption (desorption) of Fe(III) particles in Nafion® membranes by MS. This method is able to deliver really exceptional information on Fe^{2+}, Fe^{3+} ions localization, their environment in Nafion® [30] and other ionomer materials [26].

Indeed, there are great prospects to design new ion-exchange nanomaterials for various applications (electrical engineering, electronics, information technologies, biomedicine, hydrogen power) by using a combination of structural methods and MS to analyze charge states, localizations and atomic environments of magnetic iron atoms. This approach allows obtaining a valuable information for targeted synthesis and achieving the desired properties of materials.

The aim of our study was first to analyze the nanostructure of the perfluorinated membranes of Nafion®-type copolymer by complementary SAXS, determine the characteristics of ionic channels and their grouping into bunches. At the second stage of work, we tried to search subtle features of membrane ionic channels when saturated them with iron ions to examine their interactions and assembly with copolymer sulfonic groups covering the inner surface of ionic channels in membranes by optical and gamma-resonance absorption (MS) methods which gave the information on the influence of embedded iron ions on the energy of ionomer optical gap and shown the association of these ions with its sulfonic groups.

2. Experimental: samples and methods

We have synthesized perfluorinated Nafion®-type copolymer by solution copolymerization of tetrafluoroethylene (TFE) with perfluoro(3,6-dioxa-4-methyl-7-octene)sulfonyl fluoride monomer (FS-141) [43] with equivalent weight of $EW = 900$ g-eq/mol (chain fragment mass per sulfonic group SO_3H) [44]. We used the copolymer in $–SO_3Li$ form to produce the membrane films by casting method [45]. The copolymer, dissolved in dimethylformamide (DMF), was applied to a glass substrate. After the film was formed from solution by removing the solvent by heating, it was transferred to $–SO_3H$ form by washing in 15 % nitric acid, turning it into a proton-conducting membrane [45]. Then the films (60 μm, capable of water absorbing up to $\sim$ 40 wt.%) were dried and annealed at 100 °C to have stable (equilibrium) structure [45].

The dry membrane films were examined by small angle X-ray scattering (SAXS) using the BioMUR beamline (NRC Kurchatov Institute, Moscow, Russia) [46]. The SAXS intensities distributions $I(q)$ were measured in the range of scattering vector modulus $q = (4\pi/\lambda_p)\sin(\theta) = 0.04 – 4.0$ nm^{-1} for photons with wavelength λp = 0.1445 nm and scattering angle 2θ. The data corrected for background were interpreted in terms of the methodology of SAXS experiments [47].

To perform optical absorption and MS studies we saturated the films with 0.2 M $FeCl_3$ solution of followed by vacuum drying according to the method [30] to achieve the desirable iron concentration in membranes (2 wt.%). The pristine and modified membranes at ambient temperature (20 °C) were tested in the measurements of the optical density $D(\lambda)$ at light wavelengths $\lambda = 190 – 1100$ nm by the spectrophotometer DU-8600RN(PC) (Drawell Scientific, Yuzhong District, Chongqing, China).

The MS experiments were carried out on the modified samples to search the iron ions arrangement inside the conductive channels coated with SO_3H-groups, determine the ions' charge state and forms of their association with the groups at the conditions which are relatively close to those in hydrogen fuel cells [48]. The MS spectra were recorded on the

original spectrometer built at PNPI in collaboration with the Institute of Chemistry of St. Petersburg State University [49]. We have carried out the transmission measurements in fixed geometry using gamma source ^{57}Co moves in constant acceleration mode (triangular profile of Doppler velocity). We have calibrated the velocity scale against generally accepted α-Fe standard before the experiments. To process the spectra, we used the MOSSFIT program for Lorentzian line shape description. More details on the spectrometer performance can be found in recent publications [50, 51].

3. Results and discussions

3.1. SAXS studies

SAXS data for Nafion®-type copolymer ($EW = 900$ g-eq/mol) in range of scattering vector modulus $q \sim 0.04$ – 4.0 nm^{-1} (Fig. 1) corresponding to the spatial scales $2\pi/q \sim 10^0$ – 10^2 nm have revealed narrow ionic channels with transversal gyration radius $R_g < 1$ nm which are surrounded by the shells of skeletal chains with partially crystalline order and locally ordered into nanoscale bundles (domains). Indeed, the scattering intensities $I(q)$ increased at $q \leq 0.1$ nm^{-1} displayed in membrane the presence of polymer domains of $\sim 10^1$ – 10^2 nm in size (Fig. 1). At larger q we detected a local ordering of ionic channels packed into bundles with spatial period of channel arrangement $L_P \sim 2\pi/q_m$ corresponding to the position of the ionomer peak $q_m \sim 2$ nm^{-1} (Fig. 1).

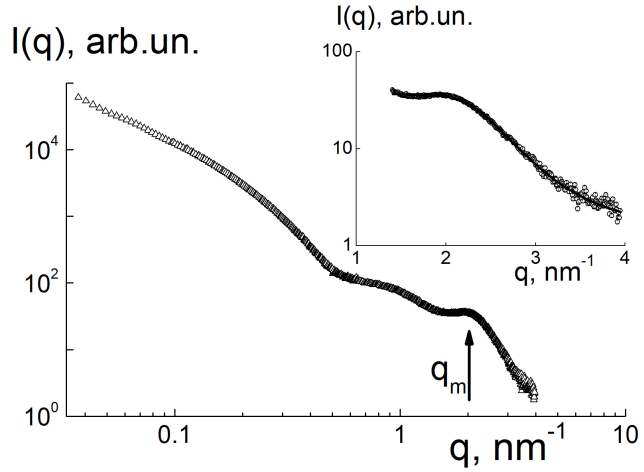

FIG. 1. SAXS intensities $I(q)$ vs. scattering vector modulus for dry Nafion® film. Ionomer peak position at q_m is indicated. Insert: ionomer peak fitting by function (1)

We used the model of thin straight ion channels being cylindrical pores with a diameter of $d_{CH} = 2\sqrt{2}R_g \sim 1$ nm much smaller than their length $L \sim 10^1$ – 10^2 nm. In the membrane, such connected linear fragments form a proton-conducting channel network. Locally these fragments are grouped into bundles of several units. This is a generally accepted model confirmed by structural data [10]. In our case, it was a principal interest to determine the structural characteristics of the channels and their mutual ordering at small scales $R \ll L$, comparable with the diameter of the channels and the transverse period of their local packing (L_P), in order to compare the data with the results of Mössbauer experiments characterizing the charge state of the iron ions in the channels when these ions interact with the surrounding sulfonic acid groups.

So, the goal was to find from the ionomer peak parameters the channel diameter corresponding to the radius R_g, their packing period L_P and at last the number in the bundle N_{CH}, which determines the transverse size of the bundle. Bundles of channels in polymer shells are elongated amorphous-crystalline polymer domains. In general, the membrane has a complex structure with alternating crystalline and amorphous regions differing in the packing density of polymer chains at the scales $R \sim 10^1$ – 10^2 nm [10]. Accordingly, on the scattering intensity curve, in addition to the ionomer peak a wide maximum weakly expressed presents at $q \sim 0.7$ nm^{-1}. It should be attributed to the contacts of bundles (domains) at a characteristic distance of $2\pi/q \sim 10$ nm of the order of their width. The length of the domains can be judged from the behavior of the scattering curve at low scattering vectors $q \leq 0.1$ nm^{-1}. In the Guinier approximation, the gyration radius of these objects is $R_G = 36 \pm 1$ nm and their length is approximately $L = \sqrt{12}R_G \approx 125$ nm as for thin rods.

The data treatment for large scattering vectors $q = 1$ – 4 nm^{-1} allowed us to evaluate the characteristics of ion channels and their arrangement using the scattering function

$$I(q) = \frac{\frac{A}{q}\exp\left[-(qR_g)^2/2\right]}{\left[1+(q-q_m)^2/\Gamma^2\right]} + \frac{B}{q}\exp\left[-\frac{(qR_g)^2}{2}\right] + Bg, \qquad (1)$$

where the first term describes the ionomer peak at $q = q_m$ with the amplitude A, full width at half maximum Γ with the factor $1/q$ which corresponds to the scattering from linear fragments of fine channels having small transversal gyration radius R_g, the second term represents the contribution of the channels when there is no interference in scattering between them and the constant Bg is the background. Note, for our dry membrane with mostly closed pores and squeezed thin ionic channels the scattering at high scattering vectors obeys asymptotic $1/q$ behavior but not $1/q^4$ for smooth (sharp) borders which really absent since in the ionic channels the terminal sulfonic groups of side chains of copolymer are contacted and overlapped that makes the borders of channels very diffuse. In this case, taking into account the atomic structure of scattering particles, using the representation of their correlation function as a sum of δ-functions, leads to the appearance of a constant component in the scattering intensity [47].

The data (Fig. 1) obeyed the function (1) with fitting parameters: $A = 125 \pm 6$ nm^{-1} arb.un., $q_m = 2.25 \pm 0.02$ nm^{-1}, $\Gamma = 0.64 \pm 0.03$ nm^{-1}, $B = 24.1 \pm 5.6$ nm^{-1} arb.un., $R_g = 0.59 \pm 0.01$ nm, $Bg = 1.58 \pm 0.10$ arb.un. The parameter R_g defines the diameter of channels, $d_{CH} = 2\sqrt{2}R_g = 1.67 \pm 0.03$ nm, that is really a characteristic size of ionic channels in such type of membranes [52]. The channels are packed with transversal period $L_P = 2\pi/q_m = 2.79 \pm 0.03$ nm which is the outer diameter of polymer shells around them. Respectively, the difference of the parameters L_C and d_{CH} gives the thickness of polymers shells, $\delta_S = (L_P - d_{CH})/2 = 0.56 \pm 0.02$ nm. This magnitude corresponds to the length of folded chain fragment between neighboring ionic groups, $nL_1/2 \approx 0.6$ nm, where $n = 4.6$ is the average number of (CF_2–CF_2) units and $L_1 \approx 0.25$ nm is their size along chain fragment. Hence, the shells around ionic channels are the assemblies of folded chain fragments like in inverted micelles [11].

As far as the parameter A is a measure of interference in scattering from neighboring channels in bundles, and the parameter B corresponds to individual scattering from linear channel fragments in bundles, the ratio of these characteristics gives the number of channels in a bundle, $N_{CH} = (A/B) + 1 = 6.1 \pm 0.1$. So, parallel channel fragments in membrane are locally gathered into the bundles while each bundle integrates about six channels that is in agreement with the structural modeling [11].

Meanwhile, in the structural analysis it should be understood that in reality, the polymer matrix is an amorphous-crystalline continuum and can only be conditionally divided into bundles (domains) scattering independently. So, the ionomer peak includes contributions not only from channels within individual bundles, but also from the channels in the nearest contacting bundles packed into a common polymer matrix. In view of this, it is not possible to attribute the parameters of the scattering function (A, B) to one or another discrete model of an isolated bundle. As a result, the average degree of channel aggregation was estimated from the found ratio A/B, and the approximate ratio $L_p = 2\pi/q_m$ was used to determine the average period of channel packing. The allocation of discrete structural levels in membranes as a result of local segregation of polar and non-polar fragments of copolymers forming a structure with nanosized amorphous-crystalline regions is conditional and does not allow developing satisfactory quantitative structural models of perfluorinated membranes. The models presented are applicable to well-oriented, highly ordered membranes that may be created in the future.

Since ionic channels with hydrophilic inner surface covered with SO_3H groups can adsorb water, in swollen state this copolymer may provide ionic transport via proton diffusion with water molecules, but protons diffuse also by Grotthuss mechanism by means of short jumps ($\sim 0.05 - 0.07$ nm) between polarized water molecules (H_3O^+), that mainly provides proton conductivity [53]. Therefore, it was important to study the ion exchange in diffusion channels of membrane. For this purpose, we saturated it with Fe^{3+} ions and measured optical absorption spectra to detect their interactions with copolymer.

3.2. Optical absorption in membranes

The absorbance spectra $D(\lambda)$ have shown the greater optical density for the membrane saturated with iron ions in the wavelength intervals 370 – 450 and 600 – 900 nm comparative to the data for pristine membrane (Fig. 2). The association of iron ions with copolymer influenced its optical gap energy (E_g). Its original magnitude $E_{g0} = 3.35 \pm 0.01$ eV became smaller by ~ 5 %. For modified material we found the energy $E_{gM} = 3.19 \pm 0.01$ eV using Tauc relation [54] between the photon energy and absorption coefficient. This relation in terms of optical density $D(\lambda)$ vs. reciprocal wavelength is as following,

$$\left[\frac{D(\lambda)}{\lambda}\right]^2 = B\left(\frac{1}{\lambda} - \frac{1}{\lambda_g}\right), \tag{2}$$

where λ_g is the wavelength corresponding to the photon energy E_g, the coefficient B depends on transition probability [55, 56]. A linear approximation of $[D(\lambda)/\lambda]^2$ vs. $1/\lambda$ has given the wavelengths $\lambda_{g0} = 370.4 \pm 0.1$ nm and $\lambda_{gM} = 389.1 \pm 0.2$ nm for original and modified membrane (Fig. 3), and corresponding magnitudes of energy gap (E_{g0}, E_{gM}) were evaluated.

The decrease in energy gap agrees with common trends in the changes of electronic properties of polyelectrolytes, e.g. for Poly(vinyl alcohol) (PVA) doped $FeCl_3$ [57]. Such kind polymer-metal composites are prospective semiconductive materials for numerous applications (optoelectronic devices, solid-state batteries, solar cells) [57–59]. In these materials, it is of crucial importance to regulate the coordination of metal atoms with ionic groups in polymer matrices. In our case, the information on iron ion assembling with sulfonic groups at channel walls was obtained in the MS experiments.

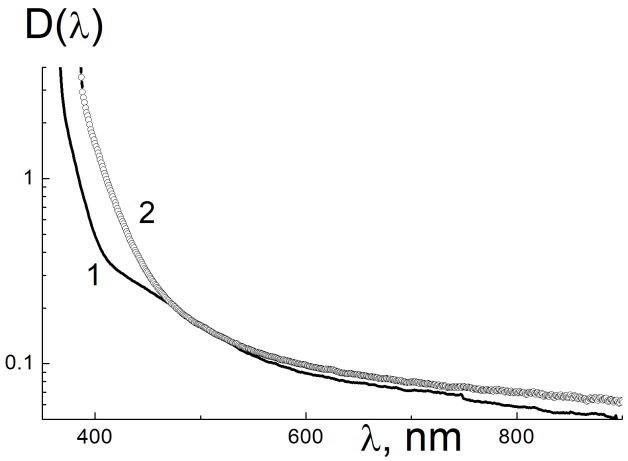

FIG. 2. Absorbance spectra $D(\lambda)$ at wavelengths 300 – 900 nm for pristine (1) and filled with Fe^{3+} membranes (2)

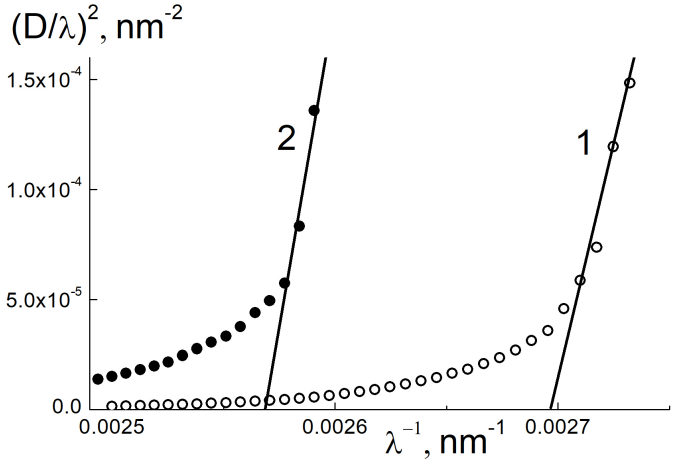

FIG. 3. Absorption data Tauc presentation for pristine (1) and filled with Fe^{3+} membranes (2), data linear approximation to find the energy of material optical gap

3.3. MS spectroscopy of membrane with iron ions

The principal feature of the experiments was a search of resonant gamma absorption in iron doped Nafion® type membranes in dry state at ambient temperature (295 K), i.e. not so far from the exploitation conditions for fuel cells. Previously we tested electrochemical properties of unfrozen membranes saturated with water and detected their high proton conductivity (0.1 S/cm). Worth to note, till now the MS spectra for iron modified Nafion® were recorded only for the samples cooled down to 80 and 4.2 K [30].

In the experiments, we performed the standard α-Fe calibration and then collected the data for membranes (4 films) gaining high statistics and detecting weak effects of gamma resonance absorption in warm sample (Fig. 4). The sample transmission $Tr(V)$ vs. source speed (V) presented in the form $\Delta Tr = (Tr - 1) = F_1 + F_2 + F_3 + F_4$ is the sum Lorentzian terms (1–4) with fitting parameters (Fig. 4, Table 1),

$$F_1(V) = \frac{A_{m1}}{\left[1 + \left(V - (IS_1 - \frac{QS_1}{2}\right)^2 / {\Gamma_{m1}}^2\right]}, \tag{3}$$

$$F_2(V) = \frac{A_{m1}}{\left[1 + \left(V - (IS_1 + \frac{QS_1}{2}\right)^2 / {\Gamma_{m1}}^2\right]}, \tag{4}$$

$$F_3(V) = \frac{A_{m2}}{\left[1 + \left(V - (IS_2 - \frac{QS_2}{2}\right)^2 / {\Gamma_{m2}}^2\right]}, \tag{5}$$

$$F_4(V) = \frac{A_{m2}}{\left[1 + \left(V - (IS_2 + \frac{QS_2}{2}\right)^2 / {\Gamma_{m2}}^2\right]}. \tag{6}$$

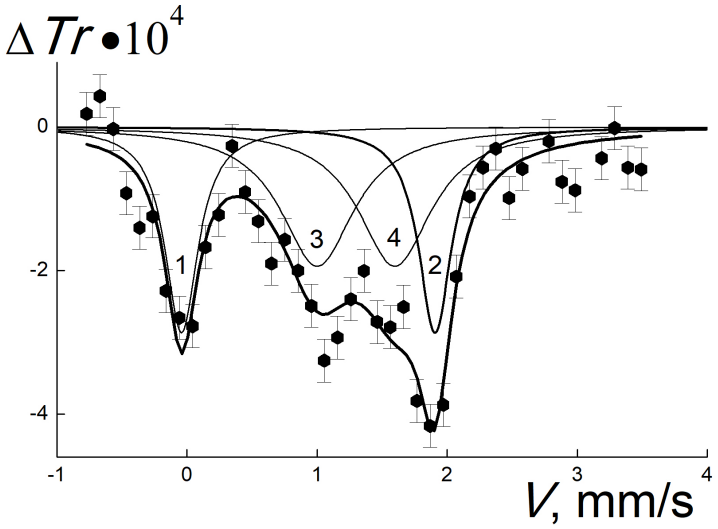

FIG. 4. Transmission data $\Delta Tr \cdot 10^4$ for gamma ray absorption in the sample vs. source speed (V), approximation by the sum of Lorentzian forms (1–4) with fitting parameters (Table 1)

TABLE 1. Spectral parameters for doublets (1,2) of gamma absorption by Fe^{3+} nuclei in membrane channels

No.	A_m, %	IS, mm/s*	QS, mm/s	Γ_m, mm/s	S, %
1	0.029 ± 0.003	0.93 ± 0.02	1.95 ± 0.03	0.31 ± 0.05	39 ± 7
2	0.020 ± 0.003	1.30 ± 0.04	0.60 ± 0.08	0.69 ± 0.14	61 ± 7

* Standard α-Fe calibration used

The data $\Delta Tr = (Tr - 1)$ demonstrated a doublet for Fe^{3+} ions but with low amplitude (~ 0.03 %) due to iron nuclei thermal motion (Fig. 4). Nevertheless, we definitely detected a quadrupole splitting of ~ 2 mm/s which was close to the magnitude ~ 1.7 mm/s for cooled Nafion® membrane ($EW = 1200$ g-eq/mol) [30]. In our case, the observed isomeric shift ~ 1 mm/s exceeded a similar effect ~ 0.6 mm/s at 80 and 4.2 K [30].

The results obtained for the first time at ambient temperature (295 K) confirmed the stability that Fe^{3+} ions ordering in membrane channels where they organize $[(H_2O)_5Fe–O–Fe(H_2O)_5]^{4+}$ dimers joint with four sulfonic acid groups (Fig. 5) to provide electro-neutrality [30]. This type dimers possess zero spin due to antiferromagnetic ordering of iron ions' spins [60, 61].

Along with the signal for dimers, the additional doublet presents in the spectrum (Fig. 4). Therefore, we fitted the data ΔTr by the sum of Lorentzian forms for doublets with amplitudes $A_{1,2}$, isomeric shifts $IS_{1,2}$, the values of quadrupole splitting $QS_{1,2}$ and linewidths $\Gamma_{1,2}$, which defined the integral contributions of doublets $S_{1,2}$ in the total absorption (Fig. 4, Table 1).

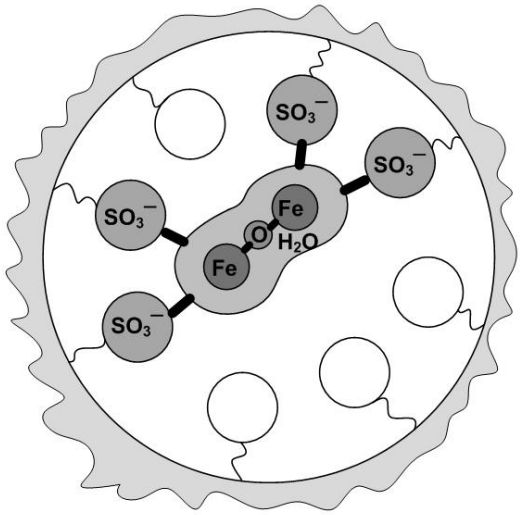

FIG. 5. Hydrated Fe^{3+} dimer associated with sulfonic acid groups in membrane ion channel

The first component has the amplitude A_1 almost one and a half times greater the A_2 for the second term, and the resonance quadrupole splitting QS_1 three times larger the QS_2 for the second signal. However, due to a bigger line width Γ_2 relative to Γ_1, the second term dominated with the ratio of integral intensities $S_2/S_1 \sim 1.6$ (Table 1). Such deviations in the parameters of the doublets reflected their different structures.

The first doublet indicated the presence of ionic dimers. However, the second doublet was attributed to $Fe(H_2O)_6^{3+}$ hydrated ions [62] with weak quadrupole splitting (~ 0.5 mm/s) [30]. At lower temperatures a bulk of them demonstrated paramagnetic hyperfine splitting since they are well separated from each other [30]. Regarding dimers, it should be clarified that in water Fe^{3+} ions are capable to form two types of clusters [30], $[(H_2O)_4Fe–(OH)_2–Fe(H_2O)_4]^{4+}$ or $[(H_2O)_5Fe–O–Fe(H_2O)_5]^{4+}$, through hydroxyls [63] or oxo-bridge [64]. The MS data [63] have shown binuclear Fe(III) oxo complex according to detected quadrupole splitting of $\sim$ 1.7 mm/s exceeding that for the entity with hydroxyls (~ 0.8 mm/s).

As the authors [30] emphasized, in Nafion®-type membranes saturated with Fe^{3+}, their dimers have the parameters identical to those in aqueous solutions. In accordance with this, in membranes at 80 and 4.2 K, the quadrupole splitting of 1.65 mm/s has indicated the presence of $[(H_2O)_5Fe–O–Fe(H_2O)_5]^{4+}$ dimers. To ensure charge neutrality for dimers, the structural model of their binding to four sulfonate groups, $[(H_2O)_5Fe–O–Fe(H_2O)_5]^{4+}[SO_3^-]_4$, was constructed based on MS and EXAFS data acquired at low temperatures [30]. However, at room temperatures in Nafion®, the effect was not detected for Fe^{3+} ions, since they were immersed in the aqueous non solid phase [62].

In the MS experiments at 295 K, we established the assembly of Fe^{3+} ions into oxo dimers coordinated with sulfonic acid groups on channel surface. We proved such a stable ionic ordering and the presence of $Fe(H_2O)_6^{3+}$ hydrated forms in warm membranes where it is possible proton migration and water diffusion in channels where dimers bridge the groups on the walls of narrow channels.

4. Conclusions

The combination of the methods of X-ray small angle scattering with optical and MS spectroscopy has expanded the experimental capabilities in perfluorinated membranes researches and allowed obtain really new unique information on the ordering of ionic groups in Nafion® type copolymer matrix with the formation of fine proton conducting channels gathered into bundles.

The discovered channel structures were based on the arrangement of sulfonic groups covering the inner surface of channels examined by MS using iron ions as tiny local probes creating dimers associated with the groups. This led also to the change in electric properties of copolymer which optical energy gap has decreased due to material modification with iron ions.

The obtained results have revealed exclusive opportunities of applied complementary methods for the examination structural, optical and electrical properties of polyelectrolytes are in demand for various applications including hydrogen power and nuclear technologies in need of effective ion exchange materials for trapping and separating nuclides.

References

[1] Ahmad S., Nawaz T., Ali A., Orhan M.F., Samreen A., Kannan A.M. An overview of proton-exchange membranes for fuel cells: Materials and manufacturing. *Int. J. of Hydrogen Energy*, 2022, **47** (44), P. 19086–19131.

[2] Pan M., Pan C., Li C., Zhao J. A review of membranes in proton exchange membrane fuel cells: Transport phenomena, performance and durability. *Renewable and Sustainable Energy Reviews*, 2021, **141** (25), 110771.

[3] Yaroslavtsev A.B., Stenina I.A. Current progress in membranes for fuel cells and reverse electrodialysis. *Mendeleev Commun.*, 2021, **31**, P. 423–432.

[4] Yaroslavtsev A.B., Stenina I.A., Golubenko D.V. Membrane materials for energy production and storage. *Pure Appl. Chem.*, 2020, **92** (7), P. 1147–1157.

[5] Li T., Shen J., Chen G., Guo S., Xie G. Performance Comparison of Proton Exchange Membrane Fuel Cells with Nafion and Aquivion Perfluorosulfonic Acids with Different Equivalent Weights as the Electrode Binders. *ACS Omega*, 2020, **5** (28), P. 17628–17636.

[6] Mugtasimova K.R., Melnikov A.P., Galitskaya E.A., Kashin A.M., Dobrovolskiy A., Don G.M., Likhomanov V.S., Sivak A.V., Sinitsyn V.V. Fabrication of Aquivion-type membranes and optimization of their elastic and transport characteristics. *Ionics*, 2018, **24**, P. 3897–3903.

[7] Dombaycıoğlu Ş, Günsel H., Aydın A.O. Nafion/Aquivion-Based Composite Lithium Ion Exchange Membranes for High Capacity Li–S Batteries. *Chemistry Select*, 2022, **7** (39), e202202910.

[8] Hsu W.Y., Gierke T.D. Ion transport and clustering in Nafion perfluorinated membranes. *J. of Membrane Science*, 1983, **13** (3), P. 307–326.

[9] Gebel G., Diat O. Neutron and X-ray scattering: Suitable tools for studying ionomer membranes. *Fuel Cells*, 2005, **5**, P. 261–276.

[10] Schmidt-Rohr K., Chen Q. Parallel cylindrical water nanochannels in Nafion fuel-cell membranes. *Nature Mater.*, 2008, **7**, P. 75–83.

[11] Fernandez Bordín S.P., Andrada H.E., Carreras A.C., Castellano G.E., Oliveira R.G., Galván Josa V.M. Nafion membrane channel structure studied by small-angle X-ray scattering and Monte Carlo simulations. *Polymer*, 2018, **155**, P. 58–63.

[12] Bazaid M., Huang Y., Goddard W.A., Jang S.S. Proton transport through interfaces in nanophase-separation of hydrated aquivion membrane: Molecular dynamics simulation approach. *Colloids and Surfaces A: Physicochemical and Engineering Aspects*, 2023, **676**, Part A, 132187.

[13] Petrov A.V., Murin I.V. Electronic Structure of SO3H Functional Groups and Proton Mobility in Nafion and Aquivion Ionomer Membranes. *Russian J. of General Chemistry*, 2019, **89** (3), P. 553–555.

[14] Agarwal T., Prasad A.K., Advani S.G., Babu S.K., Borup R.L. Infrared spectroscopy for understanding the structure of Nafion and its associated properties. *J. Mater. Chem. A*, 2024, **12**, P. 14229–14244.

[15] Mbarek S., El Kissi N., Baccouch Z., Iojoiu C. Extrusion of Nafion and Aquivion membranes: environmentally friendly procedure and good conductivities. *Polymer Bulletin*, 2019, **76**, P. 1151–1166.

[16] Haubold H.-G., Vad T., Jungbluth H., Hiller P. Nano structure of NAFION: a SAXS study. *Electrochimica Acta*, 2001, **46** (10), P. 1559–1563.

[17] Barbi V., Funari S.S., Gehrke R., Scharnagl N., Stribeck N. Nanostructure of Nafion membrane material as a function of mechanical load studied by SAXS. *Polymer*, 2003, **44**, P. 4853–4861.

[18] Elliott J.A., Wu D.S., Paddison S.J., Moore R.B. A unified morphological description of Nafion membranes from SAXS and mesoscale simulations. *Soft Matter*, 2011, **7** (15), P. 6820–6827.

[19] Xue T., Trent J.S., Osseo-Asare K. Characterization of Nafion® membranes by transmission electron microscopy. *J. of Membrane Science*, 1989, **45** (3), P. 261–271.

[20] Yakovlev S., Balsara N.P., Downing K.H. Insights on the Study of Nafion Nanoscale Morphology by Transmission Electron Microscopy. *Membranes*, 2013, **3**, P. 424–439.

[21] Yakovlev S., Downing K., Balsara N. Electron Microscopy of Nafion Membrane. *Microscopy and Microanalysis*, 2013, **19** (S2), P. 1652–1653.

[22] Aleksandrova E., Hink S., Hiesgen R., Roduner E. Spatial distribution and dynamics of proton conductivity in fuel cell membranes: Potential and limitations of electrochemical atomic force microscopy measurements. *J. of Physics: Condensed Matter*, 2011, **23** (23), 234109.

[23] Hiesgen R., Aleksandrova E., Meichsner G., Andreas Friedrich K. High-resolution imaging of ion conductivity of Nafion (R) membranes with electrochemical atomic force microscopy. *Electrochimica Acta*, 2009, **55**, P. 423–429.

[24] Tsimbal T.Yu., Chibirova F.Kh., Kostyuchenko I.G. Magnetic relaxation and submicrostructure of iron hydroxide precipitates in ionomer membrane. *J. of Magnetism and Magnetic Materials*, 1994, **136**, P. 197–203.

[25] Maksimichev A.V., Kostyuchenko I.G., Chibirova F.Kh., Zhilinskaya E.A., Chakulaeva L.N., Timashev S.F. Binding of Fe^{3+} ions to halobacterial purple membranes as studied by Mössbauer spectroscopy. *Membrane & Cell Biology*, 1997, **10** (5), P. 487–501.

[26] Chibirova F.Kh., Kostyuchenko I.G., Kirsh Yu.E. Specific features of the structure of polymer ion-exchange membranes prepared from sulfocationic aromatic polyamides as studied by Mössbauer spectroscopy. *Russian J. of Physical Chemistry*, 1999, **73** (1), P. 111–116.

[27] Cui Z., Drioli E., Lee, Y.M. Recent progress in fluoropolymers for membranes. *Progress in Polymer Science*, 2014, **39** (1), P. 164–198.

[28] Ivanchev S.S., Myakin S.V. Polymer membranes for fuel cells: manufacture, structure, modification, properties. *Russ. Chem. Rev.*, 2010, **79** (2), P. 101–117.

[29] Primachenko O.N., Marinenko E.A., Odinokov A.S., Kononova S.V., Kulvelis Yu.V., Lebedev V.T. State of the art and prospects in the development of proton?conducting perfluorinated membranes with short side chains: A review. *Polymers for Advanced Technologies*, 2021, **32** (4), P. 1386–1408.

[30] Pan H.K., Yarusso D.J., Knapp G.S., Pineri M., Meagher A., Coey J.M.D., Cooper S.L. EXAFS and Mössbauer studies of iron neutralized Nafion ionomers. *J. Chem. Phys.*, 1983, **79** (10), P. 4736–4745.

[31] Chen N., Lee Y.M. Anion exchange polyelectrolytes for membranes and ionomers. *Progress in Polymer Science*, 2021, **113**, 101345.

[32] Eisenberg A., Hird B., Moore R.B. A new multiplet-cluster model for the morphology of random ionomers. *Macromolecules*, 1990, **23** (18), P. 4098–4107.

[33] Page K.A., Cable K.M., Moore R.B. Molecular Origins of the Thermal Transitions and Dynamic Mechanical Relaxations In Perfluorosulfonate Ionomers. *Macromolecules*, 2005, **38** (15), P. 6472–6484.

[34] Wakabayashi K., Register R.A. Morphological origin of the multistep relaxation behavior in semicrystalline ethylene/methacrylic acid ionomers. *Macromolecules*, 2006, **39** (3), P. 1079–1086.

[35] Weiss R.A., Yu W.C. Viscoelastic Behavior of Very Lightly Sulfonated Polystyrene Ionomers. *Macromolecules*, 2007, **40** (10), P. 3640–3643.

[36] Mohamed H.F.M., Kobayashi Y., Kuroda C.S., Ohira A. Effects of Ion Exchange on the Free Volume and Oxygen Permeation in Nafion for Fuel Cells. *J. Phys. Chem. B*, 2009, **113** (8), P. 2247–2252.

[37] Mohamed H.F M., Kobayashi Y., Kuroda C.S., Ohira A. Free volume and gas permeation in ion-exchanged forms of the Nafion® membrane. *J. Phys. Conf. Ser.*, 2010, **225**, 012038.

[38] Ruan D., Simmons D.S. Roles of Chain Stiffness and Segmental Rattling in Ionomer Glass Formation. *J. Polym. Sci., Part B: Polym. Phys.*, 2015, **53**, P. 1458–1469.

[39] Park H.B., Nam S.Y., Rhim J.W., Lee J.M., Kim S.E., Kim J.R., Lee Y.M. Gas-transport properties through cation-exchanged sulfonatedpolysulfone membranes. *J. Appl. Polym. Sci.*, 2002, **86** (10), P. 2611–2617.

[40] Mukaddam M., Wang Y., Pinnau I. Structural, Thermal, and Gas-Transport Properties of Fe^{3+} Ion-Exchanged Nafion Membranes. *ACS Omega*, 2018, **3** (7), P. 7474–7482.

[41] Heitner-Wirguin C. Infra-red spectra of perfluorinated cation-exchanged membranes. *Polymer*, 1979, **20** (3), P. 371–374.

[42] Chen M., Ma J., Wang Z., Zhang X., Wu Z. Insights into iron induced fouling of ion-exchange membranes revealed by a quartz crystal microbalance with dissipation monitoring. *RSC Adv.*, 2017, **7**, P. 36555–36561.

[43] Odinokov A.S., Bazanova O.S., Sokolov L.F., Barabanov V.G., Timofeev S.V.Kinetics of copolymerization of tetrafluoroethylene with perfluoro(3,6-dioxa-4-methyl-7-octen)sulfonyl fluoride. *Russian J. of Applied Chemistry*, 2009, **82** (1), P. 112–115.

[44] Ivanchev S.S., Myakin S.V. Polymer membranes for fuel cells: manufacture, structure, modification, properties. *Russian Chemical Reviews*, 2010, **79** (2), P. 101–117.

[45] Primachenko O.N., Odinokov A.S., Barabanov V.G., Tyulmankov V.P., Marinenko E.A., Gofman I.V., Ivanchev S.S. Relationship between the Morphology, Nanostructure, and Strength Properties of Aquivion® Type Perfluorinated Proton-Conducting Membranes Prepared by Casting from Solution. *Russ. J. Appl. Chem.*, 2018, **91**, P. 101–104.

[46] Peters G.S., Gaponov Yu.A., Konarev P.V., Marchenkova M., Ilina K., Volkov V.V., Pisarevsky Yu.V., Kovalchuk M.V. Upgrade of the BioMUR beamline at the Kurchatov synchrotron radiation source for serial small-angle X-ray scattering experiments in solutions. *Nuclear Instruments and Methods in Physics Research Section A Accelerators Spectrometers Detectors and Associated Equipment*, 2021, **1025**, 166170.

[47] Svergun D.I., Feigin L.A. *Structure Analysis by Small-Angle X-ray and Neutron Scattering*. Plenum Press, New York, USA; London, UK, 1987, 335 p.

[48] Primachenko O.N., Kulvelis Yu.V., Odinokov A.S., Glebova N.V., Krasnova A.O., Antokolskiy L.A., Nechitailov A.A., Shvidchenko A.V., Gofman I.V., Marinenko E.A., Yevlampieva N.P., Lebedev V.T., Kuklin A.I. New Generation of Compositional Aquivion®-Type Membranes with Nanodiamonds for Hydrogen Fuel Cells: Design and Performance. *Membranes*, 2022, **12** (9), 827.

[49] Semenov V.G., Moskvin L.N., Ufimov A.A. Analytical potential of Mössbauer spectroscopy. *Russ. Chem. Rev.*, 2006, **75** (4), P. 317–327.

[50] Kamzin A.S., Obaidat I.M., Kozlov V.S., Voronina E.V., Narayanaswamy V., Al-Omari I.A. Graphene Oxide/Iron Oxide (GrO/FeOx) Nanocomposites for Biomedicine: Synthesis and Study. *Physics of the Solid State*, 2021, **63** (6), P. 856–865.

[51] Kamzin A.S., Obaidat I.M., Kozlov V.S., Voronina E.V., Narayanaswamy V., Al-Omari I.A. Magnetic Nanocomposites Graphene Oxide/Magnetite + Cobalt Ferrite (GrO/Fe_3O_4 + $CoFe_2O_4$) for Magnetic Hyperthermia. *Physics of the Solid State*, 2021, **63**, P. 998–1008.

[52] Lebedev V.T., Kulvelis Yu.V., Török Gy., Ivankov O.I., Polotskaya G.A., Vinogradova L.V., Vul A.Ya., Primachenko O.N., Marinenko E.A., Odinokov A.S. Structure of diffusive polymer membranes for molecular and ionic transport. *J. of Surface Investigation: X-ray, Synchrotron and Neutron Techniques*, 2021, **15** (5), P. 939–946. ©Pleiades Publishing, Ltd., 2021. ISSN 1027-4510.

[53] Popov I., Zhu Z., Young-Gonzales A.R., Sacci R.L., Mamontov E., Gainaru C., Paddison S.J., Sokolov A.P. Search for a Grotthuss mechanism through the observation of proton transfer. *Commun. Chem.*, 2023, **6**, 77.

[54] Tauc J., Menth A., Wood D. Optical and Magnetic Investigations of the Localized States in Semiconducting Glasses. *Phys. Rev. Lett.*, 1970, **25**, P. 749–752.

[55] Dorranian D., Abedini Z., Hojabri A., Ghoranneviss M. Structural and optical characterization of PMMA surface treated in low power nitrogen and oxygen RF plasmas. *J. of Non-Oxide Glasses*, 2009, **1** (3), P. 217–229.

[56] Mishjil K.A., Chiad S.S., Abass K., Habubi N.F. Effect of Al doping on structural and optical parameters of ZnO thin films. *Materials Focus*, 2016, **5** (5), P. 471–475.

[57] Latif D.M.A., Chiad S.S., Erhayief M.S., Abass K.H., Habubi N.F., Hussin H.A. Effects of $FeCl_3$ additives on optical parameters of PVA. *IOP Conf. Series: J. of Physics: Conf. Series*, 2018, **1003**, 012108.

[58] Reichmanis E., Donnel J.O. Irradiation of Polymeric Materials, and the Effect of Radiation on High Technology Polymers. *ACS Symposium Series*, 1993, **381** (527), 108.

[59] Omer M.A.A., Gar-elnabi M.E.M., Ahmed A.H., Eidam G.A., Khidir N.A.N. Radiochemical Properties of Irradiated PVA\$AgNO_3$ Film by Electron Beam. *Int. J. of Science and Research*, 2013, **2** (9), P. 361–364.

[60] Bauminger E.R., Levy A., Labenski de Kanter F., Ofer S., Heitner-Wirquin C. Mössbauer spectra of iron containing Nafion membranes. *J. de Physique. Colloque C1*, 1980, **41** (1), 329.

[61] Lechan R., Nicolini C., Abeledo C.R., Frankel R.B. Hyperfine Interactions in the Intramolecular Antiferromagnet (Fe salen C1)2. *J. Chem. Phys.*, 1973, **59** (6), P. 3138–3142.

[62] Rodmacq B., Pineri M., Coey J.M.D., Meagher A. Möussbauer spectroscopy of Nafion polymer membranes exchanged with Fe^{2+}, Fe^{3+}, and Eu^{3+}. *J. Polym. Sci. Polym. Phys. Ed.*, 1982, **20** (4), P. 603–619.

[63] Freitknecht W., Giovanoli R., Michaelis W., Miiller M. Über die Hydrolyse von Eisen(III)Salzlösungen. I. Die Hydrolyse der Lösungen von Eisen(III)chlorid. *Helv. Chim. Acta*, 1973, **56** (8), P. 2847–2856.

[64] Knudsen L.M., Larsen E., Moreira J.E., Nielsen O.F. Characterization of Decaaqua-mu-oxodi-iron(III) by Mössbauer and Vibrational Spectroscopy. *Acta. Chem. Scand. Sect. A*, 1975, **29** (9), P. 833–839.

Submitted 23 July 2024; revised 1 October 2024; accepted 2 October 2024

Information about the authors:

Vasily T. Lebedev – Petersburg Nuclear Physics Institute named by B. P. Konstantinov of National Research Center "Kurchatov Institute", 188300, Gatchina, Russia; ORCID 0000-0003-4894-0862; lebedev_vt@pnpi.nrcki.ru

Valery S. Kozlov – Petersburg Nuclear Physics Institute named by B. P. Konstantinov of National Research Center "Kurchatov Institute", 188300, Gatchina, Russia; kozlov_vs1@pnpi.nrcki.ru

Mikhail V. Remizov – Petersburg Nuclear Physics Institute named by B. P. Konstantinov of National Research Center "Kurchatov Institute", 188300, Gatchina, Russia; m.remizov97@gmail.com

Yury V. Kulvelis – Petersburg Nuclear Physics Institute named by B. P. Konstantinov of National Research Center "Kurchatov Institute", 188300, Gatchina, Russia; ORCID 0000-0002-3228-3039; kulvelis_yv@pnpi.nrcki.ru

Oleg N. Primachenko – Institute of Macromolecular Compounds, Russian Academy of Sciences, 199004, St. Petersburg, Russia; ORCID 0000-0003-1637-8537; alex-prima@mail.ru

Elena A. Marinenko – Institute of Macromolecular Compounds, Russian Academy of Sciences, 199004, St. Petersburg, Russia; ORCID 0000-0003-2160-2003; emarinenkospb@gmail.com

Georgy S. Peters – National Research Center "Kurchatov Institute", 123182, Moscow, Russia; ORCID 0000-0003-3597-9370; georgspeters@gmail.com

Conflict of interest: the authors declare no conflict of interest.